HHS Public Access

Author manuscript

Mol Immunol. Author manuscript; available in PMC 2021 July 01.

Published in final edited form as:

Mol Immunol. 2020 July ; 123: 97–105. doi:10.1016/j.molimm.2020.04.014.

HuR promotes miRNA-mediated upregulation of NFI-A protein expression in MDSCs during murine sepsis

Isatou Bah[1], **Tuqa Alkhateeb**[1], **Ajinkya Kumbhare**[1], **Dima Youssef**[1], **Zhi Yao**[1], **Gregory A. Hawkins**[2], **Charles E. McCall**[3], **Mohamed El Gazzar**[1,*]

[1]Department of Internal Medicine, East Tennessee State University College of Medicine, Johnson City, TN 37614, USA

[2]Department of Biochemistry and Center for Precision Medicine, Wake Forest University School of Medicine, Winston-Salem, NC 27157, USA

[3]Department of Internal Medicine, Wake Forest University School of Medicine, Winston-Salem, NC 27157, USA

Abstract

Myeloid-derived suppressor cells (MDSCs) contribute to high mortality rates during sepsis, but how sepsis induces MDSCs is unclear. Previously we reported that microRNA (miR)-21 and miR-181b reprogram MDSCs in septic mice by increasing levels of DNA binding transcription factor, nuclear factor 1 (NFI-A). Here, we provide evidence that miR-21 and miR-181b stabilize NFI-A mRNA and increase NFI-A protein levels by recruiting RNA-binding proteins HuR and Ago1 to its 3' untranslated region (3'UTR). We also find that the NFI-A GU-rich element (GRE)-binding protein CUGBP1 counters miR-21 and miR-181b dependent NFI-A mRNA stabilization and decreases protein production by replacing 3'UTR bound Ago1 with Ago2. We confirmed the miR-21 and miR-181b dependent reprogramming pathway in MDSCs transfected with a luciferase reporter construct containing an NFI-A 3'UTR fragment with point mutations in the miRNA binding sites. These results suggest that targeting NFI-A in MDSCs during sepsis may enhance resistance to uncontrolled infection.

Keywords

MDSC; Sepsis; miRNA; NFI-A

[*]**Correspondence:** Mohamed El Gazzar, Department of Internal Medicine, East Tennessee State University College of Medicine, Johnson City, TN. Tel: 423-439-8827; Fax: 423-439-6387; elgazzar@etsu.edu.

Author Statement

I.B., T.A., and A.K. performed the experiments; D.Y. and Z.Q.Y. discussed the results and commented on the manuscript; G.A.H. helped with the bioinformatic analysis; C.E.M. discussed the results and edited the manuscript; and M.E. supervised the research, and wrote the manuscript.

Conflicts of interest

None.

1. Introduction

Sepsis rapidly mobilizes innate immune cells (Cuenca *et al.*, 2011;Delano *et al.*, 2007) and may deplete myeloid cell reserves needed to resist uncontrolled infection (Cuenca *et al.*, 2011;Kelly-Scumpia *et al.*, 2010;Scumpia *et al.*, 2010). During this time, normal immune competent myeloid precursors cells deviate to myeloid-derived suppressor cells (MDSC), which suppress T cell functions as a contributing cause of disrupted innate and adaptive immune responses (Cuenca *et al.*, 2011;Mathias *et al.*, 2017;Ostrand-Rosenberg and Fenselau, 2018). We (Brudecki *et al.*, 2012a) and others (Delano *et al.*, 2007;Derive *et al.*, 2012) reported sustained expansion of $Gr1^+CD11b^+$ MDSCs in a model of murine cecal ligation and puncture (CLP) designed to simulate post-acute sepsis. Subsequently, persistent increases in MDSCs in a subset of sepsis patients contributed to a chronic post-sepsis syndrome (Mathias *et al.*, 2017;Mira *et al.*, 2017a) evidenced by increased nosocomial infections and organ dysfunction (Cuenca *et al.*, 2011;Mathias *et al.*, 2017). This post-acute sepsis (>14 d after hospitalization) increases morbidity and mortality (Hotchkiss *et al.*, 2013;Patil *et al.*, 2016;Mira *et al.*, 2017b). However, it's molecular underpinnings are unclear.

Growth factors and inflammatory mediators drive MDSC expansion under a variety of acute and chronic conditions, including infection and inflammation (Cuenca *et al.*, 2011;Ostrand-Rosenberg and Fenselau, 2018). To better understand MDSCs as contributors to sepsis outcome, we developed a mouse model of polymicrobial sepsis that reprogrammed persistent inflammation and immunosuppression (Brudecki *et al.*, 2012a). We discovered that the CCAAT-box-binding transcription factor NFI-A, which attenuates normal myeloid cell differentiation and maturation (Fazi *et al.*, 2005;Rosa *et al.*, 2007;Zardo *et al.*, 2012), expanded $Gr1^+CD11b^+$ MDSCs in bone marrow and spleens during sepsis (McPeak *et al.*, 2017). Ex vivo knockdown of NFI-A in $Gr1^+CD11b^+$ MDSCs obtained from septic mice restores their differentiation and maturation to macrophage and dendritic cells (McClure *et al.*, 2016). Conditional NFI-A knockout in the myeloid cell compartment attenuates MDSC expansion and immunosuppression and improves sepsis survival (McPeak *et al.*, 2017). We then found that microRNA (miR)-21 and miR-181b regulate NFI-A expression in $Gr1^+CD11b^+$ cells during sepsis (McClure *et al.*, 2014;McClure *et al.*, 2016). MiRNAs post-transcriptionally bind complementary sequences within the 3' untranslated region (3'UTR) of the target mRNAs (Baltimore *et al.*, 2008;O'Connell *et al.*, 2010), which assembles the repressor complex, RNA-induced silencing complex or RISC. RISC decays or represses target mRNA to downregulate protein synthesis (Baltimore *et al.*, 2008;Kim *et al.*, 2009).

In the present study, we enlighten how miR-21 and miR-181b upregulate NFI-A protein expression and MDSC development during sepsis. We found that the RNA-binding proteins HuR and CUGBP1 compete for NFI-A 3'UTR binding and either stabilize or destabilize NFI-A mRNA, and that miR-21 and miR-181b coupling to HuR increases NFI-A mRNA stability and protein levels.

2. Materials and Methods

2.1. Mice

Male BALB/c mice (8–10 weeks old) were purchased from Jackson Laboratory (Bar Harbor, ME). The mice were housed in a pathogen-free temperature-controlled room and were acclimated to the new environment for a week before surgery. All experiments were conducted in accordance with National Institutes of Health guidelines and were approved by the East Tennessee State University Animal Care and Use Committee.

We used male mice, because several clinical and experimental studies reported that cell-mediated immune responses are depressed in males with sepsis, and are unchanged or enhanced in females (Angele *et al.*, 2000;De *et al.*, 2005). Because MDSCs suppress both innate and adaptive immune responses, we exclusively used male mice in order to maximize their immunosuppressive effects during sepsis.

2.2. Sepsis model

Polymicrobial sepsis from cecal ligation and puncture (CLP) modeled MDSCs development, as described previously (Brudecki *et al.*, 2012b). Briefly, a midline abdominal incision was made, and the cecum was ligated distal to the ileocecal valve, and then punctured twice with a 23-gauge needle. A small amount of feces was extruded into the abdominal cavity. Mice received (i.p.) 1 ml lactated Ringers plus 5% dextrose for fluid resuscitation. To establish intra-abdominal infection and approximate the clinical condition of human sepsis (Mazuski *et al.*, 2002) and delay in MDSC development, mice were subcutaneously administered antibiotic (imipenem; 25 mg/kg body weight) in saline (0.9% sodium chloride) at 8 and 16 hr after CLP. This results in high mortality (~60–70%) during a post-acute sepsis phenotype (Brudecki *et al.*, 2012b). Survival was followed for 28 days. Mice moribund during acute sepsis (defined as the first 5 d after CLP) or later/chronic sepsis (post 6 d) (Brudecki *et al.*, 2012b) were euthanized and analyzed. A corresponding number of mice from the control/sham group were also analyzed at the same time point.

2.3. $Gr1^+CD11b^+$ cell isolation

$Gr1^+CD11b^+$ cells were isolated from the bone marrow by positive selection using magnetic beads (Miltenyi Biotech, Auburn, CA). Briefly, the bone marrow was flushed out of the femurs with RPMI-1640 medium (without serum) under aseptic conditions. A single cell suspension was made by pipetting up and down and filtering through a 70-μm nylon strainer, followed by incubation with erythrocyte lysis buffer and washing. The cell suspension was subjected to positive selection of the $Gr1^+$ cells by incubating with biotin-conjugated mouse anti-Gr1 antibody (Clone RB6–8C5; eBioscience, San Diego, CA) for 15 min at 4°C. Cells were then incubated with anti-biotin magnetic beads for 20 min at 4°C and subsequently passed over a MS column. The cell population was more than 90% $Gr1^+CD11b^+$ as determined by flow cytometry. $Gr1^+CD11b^+$ cells were cultured in RPMI-1640 medium (Invitrogen, Carlsbad, CA) supplemented with 100 U/ml penicillin, 100 μg/ml streptomycin, 2 mM L-glutamine (all from Hyclone Laboratories, Logan, UT), and 10% fetal bovine serum (Atlanta Biologicals, Lawrenceville, GA) at 37°C and 5% CO_2.

2.4. Cell transfection

For gene expression knockdown, pools of siRNAs specific to Ago1 (Cat #sc-44647), Ago2 (Cat #44659), HuR (Cat #sc-35620), CUGBP1 (Cat #38252), or scrambled (control) siRNAs (Cat #37007) (Santa Cruz Biotechnology) were suspended in HiPerFect reagent (Qiagen, Valencia, CA) at a 0.5 μg/ml final concentration. For miR-21 and miR-181b knockdown, mirVana miRNA inhibitors against miR-21 and miR-181b (Cat #4464084), or negative control inhibitor (Cat #4464077) (Thermo Fisher Scientific, Waltham, MA) were suspended in a HiPerFect reagent at 50 nM final concentration. The cells were incubated for 36 hr with RPMI-1640 medium.

2.5. RNA immunoprecipitation

$Gr1^+CD11b^+$ cells were subjected to formaldehyde cross-linking, to preserve native RNA-protein complexes. Briefly, the cells (~10×10^6) were washed with warm PBS and incubated with 0.2% formaldehyde (in PBS) for 10 min at room temperature. The cells were washed in cold PBS, and whole cell lysate was prepared according to published methods (Pillai *et al.*, 2005) with minor modifications, which replaced digitonin with 0.5% NP-40 and 0.5% deoxycholate, and increased incubation time to 30 min. Briefly, cross-linked lysates were incubated for 30 min on ice in lysis buffer containing: 250 mM sucrose, 10 mM Tris-HCl [pH 7.5], 25 mM KCl, 5 mM $MgCl_2$, 2 mM DTT, 0.5% NP-40, 0.5% deoxycholate, 30 U/ml RNase inhibitor, and 1x protease inhibitor cocktail (Cat #87786; Thermo Fisher Scientific, Waltham, MA). After DNase I treatment for 10 min at 37C, lysates were cleared by centrifugation at 10,000 rpm for 10 min at 4°C.

Immunoprecipitation was performed as described previously (Pillai *et al.*, 2005), except that the incubation with antibody was performed overnight. Briefly, cell lysates were pre-cleared by incubation with pre-blocked protein A/G-agarose beads for 1 h at 4°C. The beads were pre-blocked by incubation for 1 h with 100 μg/ml of BSA, and then washed with buffer C (250 mM sucrose, 10 mM Tris-HCl [pH 7.5], 25 mM KCl, 5 mM $MgCl_2$, 2 mM DTT, 30 U/ml RNase inhibitor, and 1x protease inhibitor cocktail). Cell lysate (900 μl) was added to 100 μl of pre-blocked beads that were coated with 10 μl antibody against Ago2 (clone #4G8; Wako, Richmod, VA), Ago1 (Cat #sc-376696), HuR (Cat #sc-5261), AUF1 (Cat #sc-166577), TTP (Cat #sc-374305), CUGBP1 (Cat #sc-56649), or IgG control antibody (Santa Cruz Biotechnology, Santa Cruz, CA). Samples were rotated overnight at 4°C, and the beads were centrifuged and washed three times with buffer C. Aliquots of beads-bound protein complexes were saved for protein analysis by western blot, and the remainder was subjected to RNA isolation using TRIzol reagent for mRNA immunoprecipitation or miRNeasy Mini Kit for miRNA immunoprecipitation. This RNA was used for mRNA and miRNA analysis by PCR.

2.6. Western blots

Whole cell extracts or immunoprecipitated protein complexes were resolved by electrophoresis using SDS-10% polyacrylamide gel (Bio-Rad, Hercules, CA) and transferred to nitrocellulose membranes (Thermo Fisher Scientific, Waltham, MA). Membranes were blocked with 5% milk in Tris-buffered saline/Tween-20 for 1 hr at room temperature, and then probed overnight at 4°C with pan-specific anti-NFI (Cat #sc-74444), anti-Ago1 (Cat

#sc-376696), anti-HuR (Cat #sc-5261),anti-CUGBP1 (Cat #sc-56649) (Santa Cruz Biotechnology, Santa Cruz, CA), or anti-Ago2 (clone #4G8; Wako, Richmod, VA) antibody. After washing, blots were incubated with the appropriate HRP-conjugated secondary antibody for 2 hr at room temperature. Proteins were detected with the enhanced chemiluminescence detection system (Thermo Fisher Scientific, Waltham, MA), the bands were visualized using the ChemiDoc XRS System (Bio-Rad), and the images were captured with the Image Lab Software V3.0. Membranes were stripped and reprobed with β-actin antibody (Santa Cruz) as a loading control.

2.7. Real-time PCR

Real-time PCR (RT-qPCR) was performed to determine total mRNA levels of NFI-A, as well as its levels in the immunoprecipitated RNA-protein complexes. The RNA was isolated using TRIzol reagent (Invitrogen, Carlsbad, CA), reverse transcribed and amplified using SYBR Green RT-PCR kit and QuantiTect Primer Assays specific to NFI-A (Cat #QT00121023; Qiagen, Germantown, MD) or primers that amplify the 3'UTR (Forward, 5'-ACACTTTGCTCCTCACCTAAC-3'; Reverse, 5'- CACACAGGACACTCAAGACTAC-3') (Integrated DNA Technologies, Coralville, IA). The expression level was calculated using the $2^{-\Delta\Delta Ct}$ cycle threshold. Level of GAPDH (Primer Assay Cat #QT01658692; Qiagen) was used to normalize sample input.

For miR-21 and miR-181b measurements, RNA was isolated as described above. The miRNA levels were determined by RT-qPCR using miScript SYBR Green PCR kit and miScript Primer Assays specific to miR-21 and miR-181b (Qiagen; Cat # MS00011487 and MS00032368). Level of U6 RNA (Qiagen; Cat #MS00033740) was used to normalize sample input.

2.8. Luciferase reporter assay

Our earlier analysis of NFI-A 3'UTR (McClure *et al.*, 2016) for potential miRNA binding sites using limited databases at the time (miRanda; DIANA; TargetScan), did not show any complementary miRNA matching sequences with high binding affinity. However, our most recent bioinformatic screen, using a more refined and expanded miRNA search database (miRSystem, which combines 7 target prediction programs) revealed complementary binding sites for miR-21 and miR-181b, with near-perfect match in the NFI-A mRNA 3'UTR (see Fig. 7A).

An NFI-A 3'UTR fragment (4.906 kb) that contains the miRNA binding sites (Supplementary Fig. 1) and a GU-rich element (GRE) was cloned in the pEZX-MT06 dual firefly and *Renilla* reporter vector downstream of firefly luciferase (Fig. 7). Late sepsis $Gr1^+CD11b^+$ cells were isolated from the bone marrow by positive selection and transfected (~2×10^6 cells) with 0.5 μg of luciferase plasmid (GeneCopoeia, Rockville, MD) using the HiPerFect transfection reagent per the manufacturer's instructions (Qiagen, Valencia, CA). After 48 hr, the cells were harvested, and firefly and *Renilla* luciferase activities were determined with the dual luciferase reporter assay system (Promega, Madison, WI). The pEZX-MT06 empty vector, in which the *Renilla* luciferase gene is controlled by the CMV promoter and an SV40 early enhancer promoter controls the firefly luciferase gene, served

as a control for maximum firefly luciferase gene activity. Firefly luciferase values were normalized to *Renilla* luciferase activity.

2.9. Statistical analysis

Results from at least three experiments were analyzed by Microsoft Excel, V3.0 and values were expressed as mean ± s.d. Differences among groups were analyzed by a two-tailed student's *t*-test for two groups and by a one-way ANOVA for multiple groups. *p*-values < 0.05 are shown in the figures.

3. Results

3.1. MiR-21 and miR-181b post-transcriptionally upregulate NFI-A expression.

We first assessed temporal changes in NFI-A mRNA and protein levels in $Gr1^+CD11b^+$ MDSCs isolated from septic mice at times supported by our previous report of the post-acute sepsis model (Brudecki *et al.*, 2012a). Fig. 1 shows that parallel increases in NFI-A mRNA and proteins levels align with changes in miR-21 and miR-181b expression. We then showed that combined knockdown of miR-21 and miR-181b in MDSCs from late septic mice significantly reduced both NFI-A mRNA and protein levels (Fig. 2A and B). NFI-A mRNA levels decreased in the presence of transcription inhibitor actinomycin D, resulting in a mRNA half-life of approximately 2 hr (Fig. 2C). Knockdown of miR-21 and miR-181b decreased NFI-A transcripts close to levels observed after the actinomycin D treatment.

Although NFI-A expression in $Gr1^+CD11b^+$ MDSCs is induced throughout sepsis, we focused our investigastion on late sepsis because late sepsis $Gr1^+CD11b^+$ MDSCs promote immunosuppression and chronic sepsis (Brudecki *et al.*, 2012a), which are the focus of our studies.

3.2. RNA-binding proteins Ago1 and HuR accumulate at NFI-A 3'UTR.

MiRNAs control gene expression post-transcriptionally by binding to complementary sequences within the target mRNA 3' untranslated region (3'UTR) (Filipowicz *et al.*, 2008;Keene, 2007). Since miRNAs act in conjunction with RNA-binding proteins (RBPs) (Barreau *et al.*, 2005;Fabian *et al.*, 2010;Filipowicz *et al.*, 2008), we investigated how miR-21 and miR-181b might stabilize NFI-A mRNA in MDSCs during sepsis. We first performed RNA immunoprecipitation assays to identify RBPs that may target NFI-A 3'UTR. Several RBPs are commonly involved in post-transcriptional gene regulation, including Ago1, Ago2, AUF1, HuR, CUGBP1 and TTP (Barreau *et al.*, 2005;Fabian *et al.*, 2010;Keene, 2007).

Real-time PCR analysis of the immunoprecipitated RNA- using primers specific to the NFI-A 3'UTR- identified significantly higher levels of NFI-A mRNA only in Ago1- and HuR-immunoprecipitated protein complexes compared with the IgG-immunoprecipitated samples (Fig. 3A). To test whether miR-21 and miR-181b recruit RNA binding proteins (RBP) to NFI-A 3'UTR, we performed immunoprecipitation after miR-21 and miR-181b knockdown. Fig 3B shows that Ago1 and HuR levels decreased concurrent with increased Ago2 and CUGBP1 bindings. Ago1 or HuR knockdown decreased total NFI-A mRNA and protein

(Fig. 3C and D), and Ago2 and CUGBP1 replaced Ago1 and HuR proteins when we depleted miR-21 and miR-181b. Changes in Ago1 and HuR did not affect each other's gene expression (Fig. 3E). Ago1/HuR and CUGBP1/Ago2 exchange also occurred in MDSCs during early sepsis (Supplementary Fig. 2).

3.3. HuR loads miR-21 and miR-181b on the NFI-A 3'UTR.

Because knockdown of miR-21 and miR-181b decreased HuR and Ago1 protein bindings at the NFI-A 3'UTR (Fig. 3B), we examined the kinetics of the miRNA interactions with HuR and Ago1 by measuring their association with Ago1 and HuR, using RNA immunoprecipitation assay. Fig. 4A and B show that miR-21 and miR-181b enrich in HuR or in Ago1 immunoprecipitates. Then, we tested whether HuR and/or Ago1 facilitates miR-21 and miR-181b loading on NFI-A 3'UTR using HuR or Ago1 knockdown. MiR-21 and miR-181b associated with HuR before and after Ago1 knockdown, but their levels decreased significantly in Ago1 immunoprecipitated protein complexes after HuR knockdown (Fig. 4C and D). Total cellular miR-21 and miR-181b levels did not change (Fig. 4E), and HuR co-immunoprecipitated with Ago1 (Fig. 4F).

3.4. CUGBP1 destabilizes NFI-A mRNA.

We then assessed whether CUGBP1 associates with NFI-A mRNA 3'UTR and miR-21 and miR-181b after HuR knockdown in MDSCs. Fig. 5A shows that HuR knockdown facilitated CUGBP1 binding to NFI-A 3'UTR and decreased NFI-A protein levels. Meantime, miR-21 and miR-181b were not detected in the CUGBP1 immunoprecipitated protein complexes, either before or after HuR knockdown (Fig. 5B), indicating that miR-21 and miR-181b do not bind to CUGBP1 protein. In addition, co-immunoprecipitation revealed that CUGBP1 and Ago2 form a protein complex only in the absence of HuR (Fig. 5C). We next examined whether miR-21 and miR-181b can bind to Ago2 protein directly. Fig. 5D shows no miRNAs in Ago2 immunoprecipitates, either in the presence or absence of CUGBP1. In addition, levels of cellular NFI-A mRNA increased significantly after CUGBP1 knockdown (Fig. 5E).

3.5. CUGBP1 binds NFI-A 3'UTR directly.

We determined whether CUGBP1 and Ago2 formed a protein complex. We found CUGBP1 and Ago2 formed a protein complex only after the miRNA knockdown (Fig. 6A), which also bound to the NFI-A 3'UTR (Fig. 6B) and paralleled a decrease in NFI-A protein levels (right panel). We then examined whether CUGBP1 and Ago2 bind to NFI-A 3'UTR after combined knockdown of the miRNAs, CUGBP1 and Ago2. The results showed unbound Ago2 in the absence of CUGBP1 (Fig. 6C). In contrast, CUGBP1 binding was not affected by Ago2 knockdown (Fig. 6D) and NFI-A protein levels remained the same with either knockdown.

3.6. MiR-21 and miR-181b upregulate reporter mRNA expression.

We used a NFI-A 3'UTR reporter construct to assess the effect of miR-21 and miR-181b binding sites. A 3'UTR fragment (4.906 kb) that contains the miRNA binding sites and a GU-rich element (GRE) was cloned in a dual firefly and *Renilla* reporter vector downstream

of firefly luciferase (Fig. 7 A and B). Fig. 7C shows that the 3'UTR fragment containing the native miR-21 and miR-181b binding sites along with the GRE element only slightly increased the luciferase reporter expression compared with a control reporter without the NFI-A 3'UTR. In contrast, point mutations in the miR-21 and miR-181b sites decreased luciferase expression, and deleting the GRE sequence while retaining native miRNA binding sites restored the luciferase gene expression.

4. Discussion

The major finding of this study is that miR-21 and miR-181b promote MDSC development in murine sepsis in part by a post-transcriptional regulation of NFI-A. The post-transcriptional process involves HuR and Ago1 binding to NFI-A 3'UTR. RNA-binding protein CUGBP1 binding to NFI-A 3'UTR in the absence of HuR destabilizes NFI-A mRNA concomitant with exchanging Ago2 and Ago1. The data add a pivotal 3'UTR post-transcriptional mechanism previously unreported to transcriptional and epigenetic control over MDSC development during sepsis (Hollen *et al.*, 2019). The emerging mechanisms that control MDSC development and circulation during murine sepsis, if confirmed in human studies, may inform molecular targeting of human MDSCs.

The inflammatory environment of sepsis caused by accumulation of $Gr1^{+}CD11b^{+}$ MDSCs mutes inflammatory autotoxicity, but concomitantly limits the host clearance of the unresolved original or new infection (Brudecki *et al.*, 2012a;Cuenca *et al.*, 2011;Mathias *et al.*, 2017). Our previous data indicated that NFI-A transcription factor maintains an undifferentiated state (McClure *et al.*, 2016) and promotes MDSCs during sepsis (McPeak *et al.*, 2017) by mechanisms dependent on increased miR-21 and miR-181b expression, but more precise molecular mapping remained unclear. One possibility is control over mRNA coupling at 3'UTR to protein expression. The NFI-A 3'UTR contains consensus sequences complementary to miR-21 and miR-181b "seed" regions. In this study we showed that miR-21 and miR-181b assemble HuR and Ago1 RBPs at the NFI-A 3'UTR. While some studies support that miRNAs downregulate target mRNA expression by inducing mRNA decay or translation repression (Chekulaeva and Filipowicz, 2009;Filipowicz, 2005), other stress that miRNA can upregulate target mRNA expression by increasing mRNA stability (Del *et al.*, 2016;Mortensen *et al.*, 2011;Prislei *et al.*, 2013;Vasudevan *et al.*, 2007). In this study, HuR stabilized NFI-A mRNA in sepsis MDSCs and complexed with Ago1 at NFI-A 3'UTR. Ago1 knockdown, a known mRNA regulatory protein in mammalian cells (Ambros, 2004;Filipowicz, 2005), did not alter miRNAs association with HuR, which post-transcriptionally stabilizes mRNAs of many genes (Abdelmohsen and Gorospe, 2010;Lebedeva *et al.*, 2011;Simone and Keene, 2013). Although the exact mechanism by which HuR promotes target mRNA stability is not completely understood, some studies suggest that HuR competes with other RBPs that promote mRNA degradation (Abdelmohsen and Gorospe, 2010). If so, HuR might be part of a post-transcriptional axis that contributes to sepsis homeostasis dysregulation of inflammatory mediators (El Gazzar, 2014;McCall *et al.*, 2011).

In support of the axis concept, this study showed that the CUG-binding protein CUGBP1, unlike HuR, destabilizes NFI-A mRNA whereas HuR stabilizes NFI-A mRNA. CUGBP1

binds to GU-rich sequences in target mRNAs to promote rapid decay (Rattenbacher *et al.*, 2010;Vlasova and Bohjanen, 2008). The NFI-A 3'UTR contains a 45-nt GU-rich sequence (with 8 GU-rich elements) downstream of miR-181b binding site. In this study, CUGBP1 bound to Ago2 at NFI-A 3'UTR. Ago2 catalyzes endoribonucleolytic cleavage of target mRNA, leading to its degradation (Chen *et al.*, 2009;Meister *et al.*, 2004). We suggest that miR-21 and miR-181b may promote NFI-A expression post-transcriptionally by decreasing mRNA destabilization by CUGBP1. The implication of this study is whether similar switch contributes to the immune resistance to immune tolerance phenotypes of human sepsis.

In summary, this study reveals a newly described post-transcriptional concept for myeloid cell differentiation to the MDSC phenotype, in which the HuR and CUGBP1 axis informs miR-21 and miR-181b control over NFI-A protein support of MDSC development. Mechanistically, HuR stabilizes NFI-A mRNA to increase protein, and CUGBP1 destabilizes NFI-A mRNA to decrease protein. This unrecognized pivot may inform druggable targets and improve understanding of sustained MDSC expansion during the post-sepsis syndrome of persistent inflammation and catabolism (Gentile *et al.*, 2012;Mathias *et al.*, 2017).

Supplementary Material

Refer to Web version on PubMed Central for supplementary material.

Acknowledgements

This work was supported by National Institutes of Health Grant R01GM103887 (to ME).

Reference

1. Abdelmohsen K, Gorospe M, 2010 Posttranscriptional regulation of cancer traits by HuR. Wiley. Interdiscip. Rev. RNA 1, 214–229. [PubMed: 21935886]
2. Ambros V, 2004 The functions of animal microRNAs. Nature 431, 350–355. [PubMed: 15372042]
3. Angele MK, Schwacha MG, Ayala A, Chaudry IH, 2000 Effect of gender and sex hormones on immune responses following shock. Shock 14, 81–90. [PubMed: 10947147]
4. Baltimore D, Boldin MP, O'Connell RM, Rao DS, Taganov KD, 2008 MicroRNAs: new regulators of immune cell development and function. Nat. Immunol 9, 839–845. [PubMed: 18645592]
5. Barreau C, Paillard L, Osborne HB, 2005 AU-rich elements and associated factors: are there unifying principles? Nucleic Acids Res. 33, 7138–7150. [PubMed: 16391004]
6. Brudecki L, Ferguson DA, McCall CE, El Gazzar M, 2012a Myeloid-derived suppressor cells evolve during sepsis and can enhance or attenuate the systemic inflammatory response. Infect. Immun 80, 2026–2034. [PubMed: 22451518]
7. Brudecki L, Ferguson DA, Yin D, Lesage GD, McCall CE, El Gazzar M, 2012b Hematopoietic stem-progenitor cells restore immunoreactivity and improve survival in late sepsis. Infect. Immun 80, 602–611. [PubMed: 22144495]
8. Chekulaeva M, Filipowicz W, 2009 Mechanisms of miRNA-mediated post-transcriptional regulation in animal cells. Curr. Opin. Cell Biol 21, 452–460. [PubMed: 19450959]
9. Chen CY, Zheng D, Xia Z, Shyu AB, 2009 Ago-TNRC6 triggers microRNA-mediated decay by promoting two deadenylation steps. Nat. Struct. Mol. Biol 16, 1160–1166. [PubMed: 19838187]
10. Cuenca AG, Delano MJ, Kelly-Scumpia KM, Moreno C, Scumpia PO, Laface DM, Heyworth PG, Efron PA, Moldawer LL, 2011 A paradoxical role for myeloid-derived suppressor cells in sepsis and trauma. Mol. Med 17, 281–292. [PubMed: 21085745]

11. De MA, Torres MB, Reeves RH, 2005 Genetic determinants influencing the response to injury, inflammation, and sepsis. Shock 23, 11–17. [PubMed: 15614125]
12. Del VG, De VF, Saunders SJ, Risi A, Mannironi C, Bozzoni I, Presutti C, 2016 RNA-binding protein HuR and the members of the miR-200 family play an unconventional role in the regulation of c-Jun mRNA. RNA. 22, 1510–1521. [PubMed: 27473170]
13. Delano MJ, Scumpia PO, Weinstein JS, Coco D, Nagaraj S, Kelly-Scumpia KM, O'Malley KA, Wynn JL, Antonenko S, Al-Quran SZ, Swan R, Chung CS, Atkinson MA, Ramphal R, Gabrilovich DI, Reeves WH, Ayala A, Phillips J, Laface D, Heyworth PG, Clare-Salzler M, Moldawer LL, 2007 MyD88-dependent expansion of an immature GR-1(+)CD11b(+) population induces T cell suppression and Th2 polarization in sepsis. J. Exp. Med 204, 1463–1474. [PubMed: 17548519]
14. Derive M, Bouazza Y, Alauzet C, Gibot S, 2012 Myeloid-derived suppressor cells control microbial sepsis. Intensive Care Med. 38, 1040–1049. [PubMed: 22552586]
15. El Gazzar M, 2014 microRNAs as potential regulators of myeloid-derived suppressor cell expansion. Innate. Immun 20, 227–238. [PubMed: 23757323]
16. Fabian MR, Sonenberg N, Filipowicz W, 2010 Regulation of mRNA translation and stability by microRNAs. Annu. Rev. Biochem 79, 351–379. [PubMed: 20533884]
17. Fazi F, Rosa A, Fatica A, Gelmetti V, De Marchis ML, Nervi C, Bozzoni I, 2005 A minicircuitry comprised of microRNA-223 and transcription factors NFI-A and C/EBPalpha regulates human granulopoiesis. Cell 123, 819–831. [PubMed: 16325577]
18. Filipowicz W, 2005 RNAi: the nuts and bolts of the RISC machine. Cell 122, 17–20. [PubMed: 16009129]
19. Filipowicz W, Bhattacharyya SN, Sonenberg N, 2008 Mechanisms of post-transcriptional regulation by microRNAs: are the answers in sight? Nat. Rev. Genet 9, 102–114. [PubMed: 18197166]
20. Gentile LF, Cuenca AG, Efron PA, Ang D, Bihorac A, McKinley BA, Moldawer LL, Moore FA, 2012 Persistent inflammation and immunosuppression: a common syndrome and new horizon for surgical intensive care. J. Trauma Acute. Care Surg 72, 1491–1501. [PubMed: 22695412]
21. Hollen MK, Stortz JA, Darden D, Dirain ML, Nacionales DC, Hawkins RB, Cox MC, Lopez MC, Rincon JC, Ungaro R, Wang Z, Wu Q, Brumback B, Gauthier ML, Kladde M, Leeuwenburgh C, Segal M, Bihorac A, Brakenridge S, Moore FA, Baker HV, Mohr AM, Moldawer LL, Efron PA, 2019 Myeloid-derived suppressor cell function and epigenetic expression evolves over time after surgical sepsis. Crit Care 23, 355. [PubMed: 31722736]
22. Hotchkiss RS, Monneret G, Payen D, 2013 Sepsis-induced immunosuppression: from cellular dysfunctions to immunotherapy. Nat. Rev. Immunol 13, 862–874. [PubMed: 24232462]
23. Keene JD, 2007 RNA regulons: coordination of post-transcriptional events. Nat. Rev. Genet 8, 533–543. [PubMed: 17572691]
24. Kelly-Scumpia KM, Scumpia PO, Delano MJ, Weinstein JS, Cuenca AG, Wynn JL, Moldawer LL, 2010 Type I interferon signaling in hematopoietic cells is required for survival in mouse polymicrobial sepsis by regulating CXCL10. J. Exp. Med 207, 319–326. [PubMed: 20071504]
25. Kim VN, Han J, Siomi MC, 2009 Biogenesis of small RNAs in animals. Nat. Rev. Mol. Cell Biol 10, 126–139. [PubMed: 19165215]
26. Lebedeva S, Jens M, Theil K, Schwanhausser B, Selbach M, Landthaler M, Rajewsky N, 2011 Transcriptome-wide analysis of regulatory interactions of the RNA-binding protein HuR. Mol. Cell 43, 340–352. [PubMed: 21723171]
27. Mathias B, Delmas AL, Ozrazgat-Baslanti T, Vanzant EL, Szpila BE, Mohr AM, Moore FA, Brakenridge SC, Brumback BA, Moldawer LL, Efron PA, 2017 Human Myeloid-derived Suppressor Cells are Associated With Chronic Immune Suppression After Severe Sepsis/Septic Shock. Ann. Surg 265, 827–834. [PubMed: 27163951]
28. Mazuski JE, Sawyer RG, Nathens AB, DiPiro JT, Schein M, Kudsk KA, Yowler C, 2002 The Surgical Infection Society guidelines on antimicrobial therapy for intra-abdominal infections: an executive summary. Surg. Infect. (Larchmt.) 3, 161–173. [PubMed: 12542922]

29. McCall CE, El Gazzar M, Liu T, Vachharajani V, Yoza B, 2011 Epigenetics, bioenergetics, and microRNA coordinate gene-specific reprogramming during acute systemic inflammation. J. Leukoc. Biol 90, 439–446. [PubMed: 21610199]
30. McClure C, Ali E, Youssef D, Yao ZQ, McCall CE, El Gazzar M, 2016 NFI-A disrupts myeloid cell differentiation and maturation in septic mice. J. Leukoc. Biol 99, 201–211. [PubMed: 26259914]
31. McClure C, Brudecki L, Ferguson DA, Yao ZQ, Moorman JP, McCall CE, El Gazzar M, 2014 MicroRNA 21 (miR-21) and miR-181b couple with NFI-A to generate myeloid-derived suppressor cells and promote immunosuppression in late sepsis. Infect. Immun 82, 3816–3825. [PubMed: 24980967]
32. McPeak MB, Youssef D, Williams DA, Pritchett C, Yao ZQ, McCall CE, El Gazzar M, 2017 Myeloid Cell-Specific Knockout of NFI-A Improves Sepsis Survival. Infect. Immun 85.
33. Meister G, Landthaler M, Patkaniowska A, Dorsett Y, Teng G, Tuschl T, 2004 Human Argonaute2 mediates RNA cleavage targeted by miRNAs and siRNAs. Mol. Cell 15, 185–197. [PubMed: 15260970]
34. Mira JC, Gentile LF, Mathias BJ, Efron PA, Brakenridge SC, Mohr AM, Moore FA, Moldawer LL, 2017a Sepsis Pathophysiology, Chronic Critical Illness, and Persistent Inflammation-Immunosuppression and Catabolism Syndrome. Crit Care Med. 45, 253–262. [PubMed: 27632674]
35. Mira JC, Gentile LF, Mathias BJ, Efron PA, Brakenridge SC, Mohr AM, Moore FA, Moldawer LL, 2017b Sepsis Pathophysiology, Chronic Critical Illness, and Persistent Inflammation-Immunosuppression and Catabolism Syndrome. Crit Care Med. 45, 253–262. [PubMed: 27632674]
36. Mortensen RD, Serra M, Steitz JA, Vasudevan S, 2011 Posttranscriptional activation of gene expression in Xenopus laevis oocytes by microRNA-protein complexes (microRNPs). Proc. Natl. Acad. Sci. U. S. A 108, 8281–8286. [PubMed: 21536868]
37. O'Connell RM, Rao DS, Chaudhuri AA, Baltimore D, 2010 Physiological and pathological roles for microRNAs in the immune system. Nat. Rev. Immunol 10, 111–122. [PubMed: 20098459]
38. Ostrand-Rosenberg S, Fenselau C, 2018 Myeloid-Derived Suppressor Cells: Immune-Suppressive Cells That Impair Antitumor Immunity and Are Sculpted by Their Environment. J. Immunol 200, 422–431. [PubMed: 29311384]
39. Patil NK, Bohannon JK, Sherwood ER, 2016 Immunotherapy: A promising approach to reverse sepsis-induced immunosuppression. Pharmacol. Res 111, 688–702. [PubMed: 27468649]
40. Pillai RS, Bhattacharyya SN, Artus CG, Zoller T, Cougot N, Basyuk E, Bertrand E, Filipowicz W, 2005 Inhibition of translational initiation by Let-7 MicroRNA in human cells. Science 309, 1573–1576. [PubMed: 16081698]
41. Prislei S, Martinelli E, Mariani M, Raspaglio G, Sieber S, Ferrandina G, Shahabi S, Scambia G, Ferlini C, 2013 MiR-200c and HuR in ovarian cancer. BMC. Cancer 13, 72. [PubMed: 23394580]
42. Rattenbacher B, Beisang D, Wiesner DL, Jeschke JC, von HM, St Louis-Vlasova IA, Bohjanen PR, 2010 Analysis of CUGBP1 targets identifies GU-repeat sequences that mediate rapid mRNA decay. Mol. Cell Biol 30, 3970–3980. [PubMed: 20547756]
43. Rosa A, Ballarino M, Sorrentino A, Sthandier O, De Angelis FG, Marchioni M, Masella B, Guarini A, Fatica A, Peschle C, Bozzoni I, 2007 The interplay between the master transcription factor PU.1 and miR-424 regulates human monocyte/macrophage differentiation. Proc. Natl. Acad. Sci. U. S. A 104, 19849–19854. [PubMed: 18056638]
44. Scumpia PO, Kelly-Scumpia KM, Delano MJ, Weinstein JS, Cuenca AG, Al-Quran S, Bovio I, Akira S, Kumagai Y, Moldawer LL, 2010 Cutting edge: bacterial infection induces hematopoietic stem and progenitor cell expansion in the absence of TLR signaling. J. Immunol 184, 2247–2251. [PubMed: 20130216]
45. Simone LE, Keene JD, 2013 Mechanisms coordinating ELAV/Hu mRNA regulons. Curr. Opin. Genet. Dev 23, 35–43. [PubMed: 23312841]
46. Vasudevan S, Tong Y, Steitz JA, 2007 Switching from repression to activation: microRNAs can upregulate translation. Science 318, 1931–1934. [PubMed: 18048652]

47. Vlasova IA, Bohjanen PR, 2008 Posttranscriptional regulation of gene networks by GU-rich elements and CELF proteins. RNA. Biol 5, 201–207. [PubMed: 18971639]

48. Zardo G, Ciolfi A, Vian L, Starnes LM, Billi M, Racanicchi S, Maresca C, Fazi F, Travaglini L, Noguera N, Mancini M, Nanni M, Cimino G, Lo-Coco F, Grignani F, Nervi C, 2012 Polycombs and microRNA-223 regulate human granulopoiesis by transcriptional control of target gene expression. Blood 119, 4034–4046. [PubMed: 22327224]

Highlights

- A mechanism for miRNA-mediated upregulation of NFI-A in MDSCs during sepsis is proposed.
- HuR couples with miR-21 and miR-181b to stabilize NFI-A mRNA and increases its protein level in MDSCs.
- CUGBP1 destabilizes NFI-A mRNA in the absence of miR-21 and miR-181b.

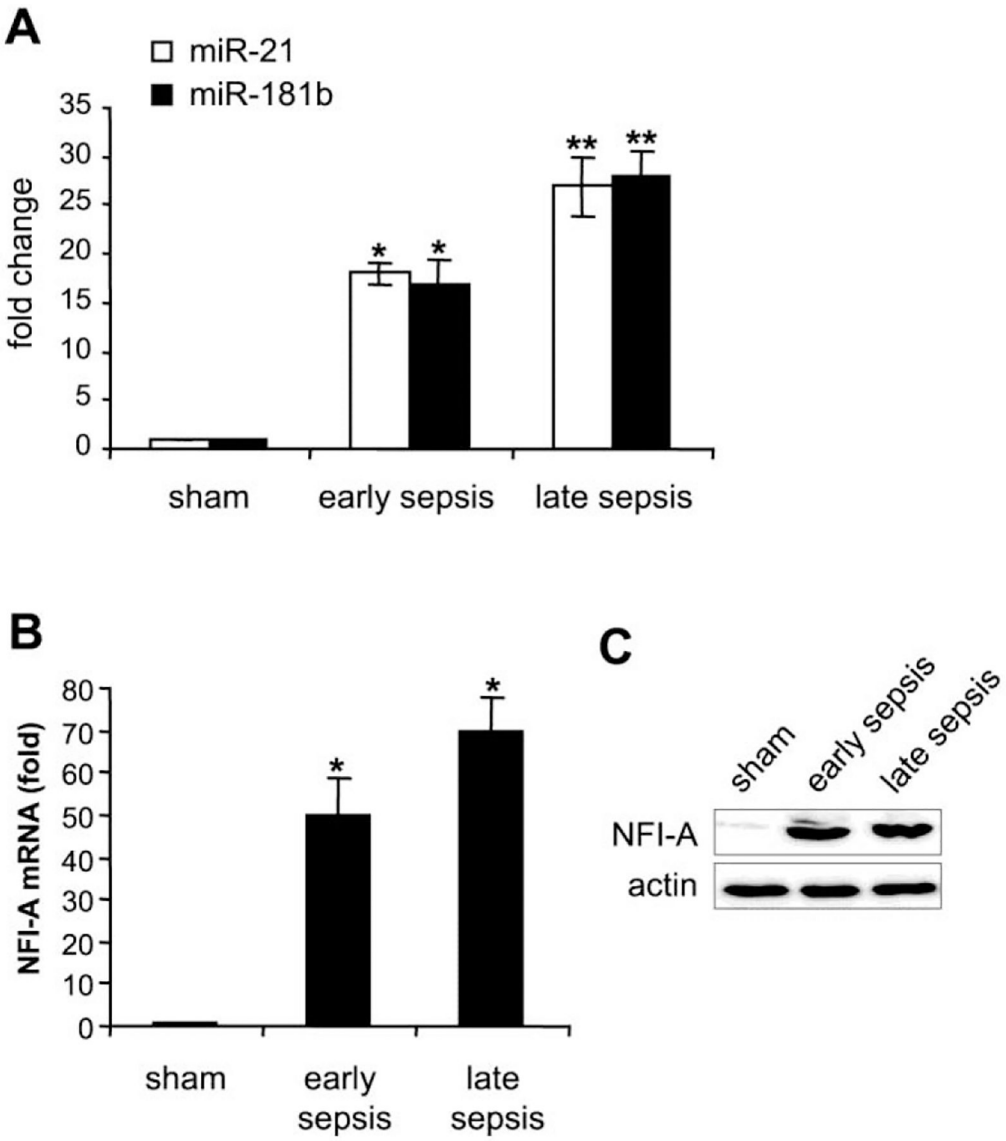

Figure 1: Correlation of NFI-A, miR-21 and miR-181b expressions in $Gr1^+CD11b^+$ myeloid cells during sepsis.

$Gr1^+CD11b^+$ cells were isolated from the bone marrow of sham and septic mice by positive selection. **(A)** Total RNA was isolated using RNeasy kit, and levels of miR-21 and miR-181b were determined by RT-qPCR using miScript SYBR Green PCR kit and assay primers specific to miR-21 and miR-181b. The miRNA expression was normalized to U6 RNA as an internal control. **(B)** NFI-A mRNA levels determined by RT-qPCR were normalized to GAPDH mRNA. Data in *A* and *B* are means ± SD of three experiments (n = 6–9 mice per group) and are presented relative to sham (1-fold). *$p < 0.05$ vs. sham; **$p < 0.05$ vs. early sepsis. (**C**) Levels of NFI-A proteins in whole cell lysates were determined by western blot using anti-NFI antibody. The results are representative of three experiments.

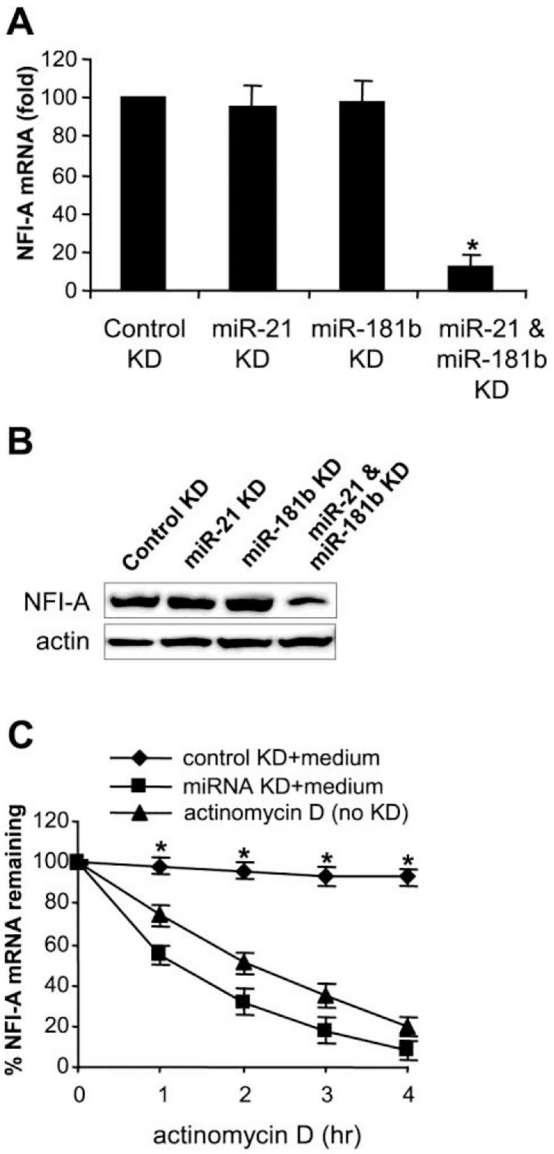

Figure 2: Effects of deleting miR-21 and miR-181b on NFI-A mRNA decay in sepsis Gr1$^+$CD11b$^+$ cells.

(A) To assess NFI-A mRNA, Gr1$^+$CD11b$^+$ cells isolated from the bone marrow of late septic mice were transfected with miR-21 and/or miR-181b inhibitor, or negative controls, and cultured for 36 hr. RNA was quantified by RT-qPCR and normalized to GAPDH mRNA. Data are means ± SD of three experiments (n = 6–7 mice per group) and are presented relative to control KD. *$p < 0.05$. **(B)** To assess NFI-A protein levels, whole cell lysates were probed by western blot using anti-NFI antibody. The results are representative of two experiments. (**C**) To determine NFI-A mRNA half-life, Gr1$^+$CD11b$^+$ cells were incubated for the indicated times with or without 5 μg/ml actinomycin D to stop mRNA transcription. NFI-A mRNA was assessed by RT-qPCR as in *A*. Data are means ± SD from 4 cultures and are presented relative to control KD. *$p < 0.05$ vs. miRNA KD + medium or actinomycin D. KD, knockdown.

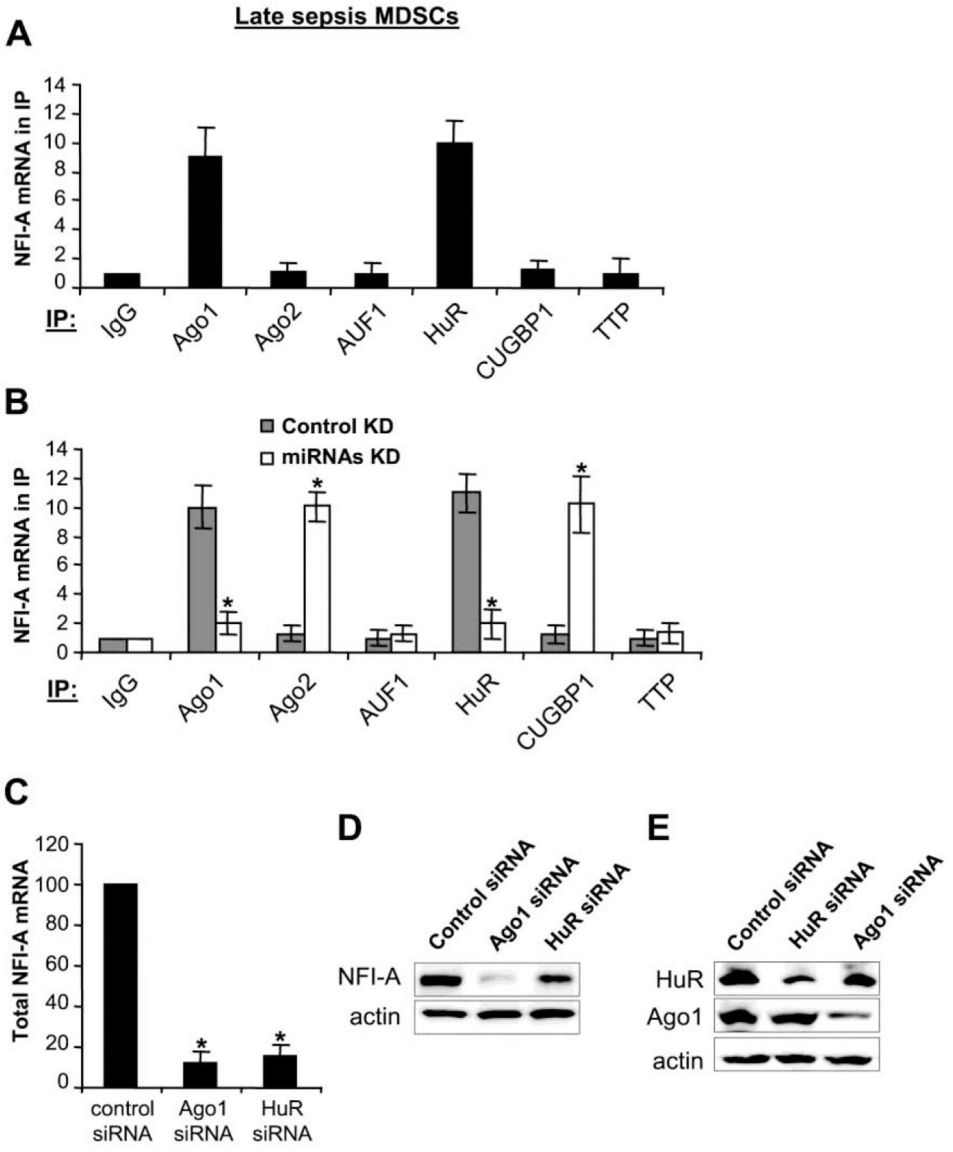

Figure 3: Binding of RNA regulatory proteins to NFI-A mRNA in sepsis Gr1$^+$CD11b$^+$ cells.

Gr1$^+$CD11b$^+$ cells were isolated from the bone marrow of late septic mice. **(A)** Ago1 and HuR bind to NFI-A mRNA. Whole cell lysates were immunoprecipitated using A/G-agarose beads coated with antibody against Ago1, Ago2, HuR, AUF1, TTP, CUGBP1 or IgG isotype control antibody. RNA was extracted from the immunoprecipitates (IP) and analyzed by RT-qPCR for the presence of NFI-A mRNA using primers that amplify the 3'UTR sequence. Values were normalized to GAPDH mRNA. **(B)** To assess Ago1 and HuR bindings to NFI-A mRNA in the absence of miR-21 and miR-181b, the Gr1$^+$CD11b$^+$ cells were transfected with miR-21 and miR-181b inhibitors or negative control inhibitors, and cultured for 36 hr. Cell lysates were prepared, immunoprecipitated, and NFI-A mRNA was measured as in *A*. Data are means ± SD of three experiments (n = 5–6 mice per group) and are presented relative to IgG IP (1-fold). *$p < 0.05$ vs. control KD. **(C)** NFI-A mRNA and protein levels after Ago1 or HuR knockdown. The Gr1$^+$CD11b$^+$ cells were transfected with Ago1-, HuR-

specific or control siRNAs and cultured for 36 hr. Total RNA was isolated using TRIzol reagent, and levels of cellular NFI-A mRNA were measured by RT-qPCR and normalized to GAPDH mRNA. Data are means ± SD of three experiments (n = 6–8 mice per group) and are presented relative to control siRNA (100%). *$p < 0.05$ vs. control siRNA. **(D)** Levels of NFI-A protein were determined by western blot using anti-NFI antibody. **(E)** Ago1 and HuR do not affect each other expression. Levels of Ago1 and HuR proteins were determined by western blot. The results are representative of two experiments. KD, knockdown.

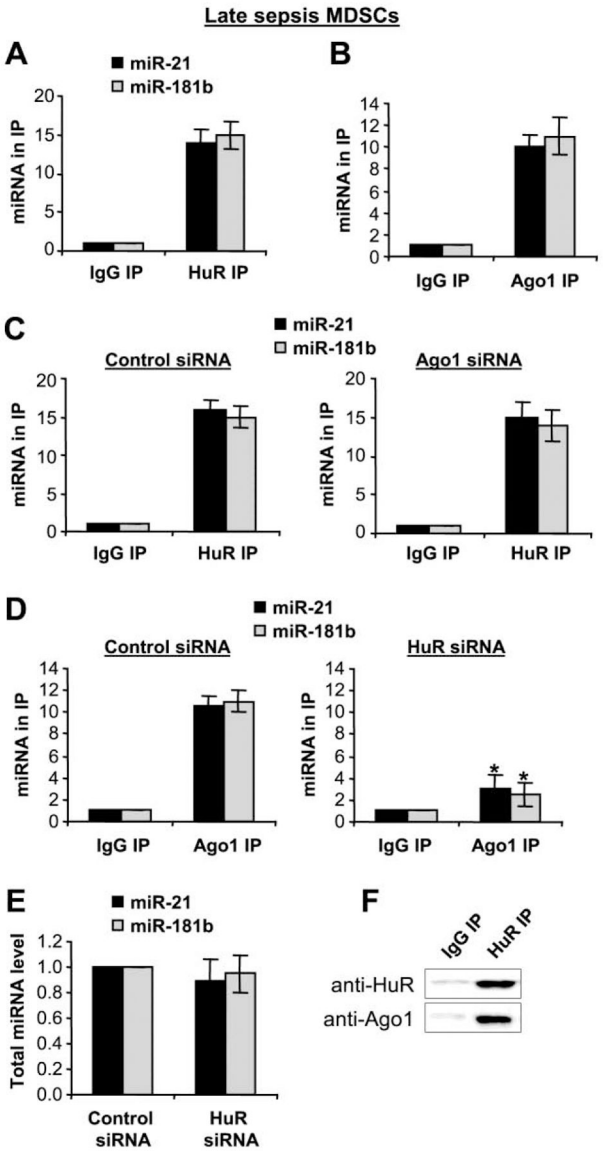

Figure 4: HuR effect on the miR-21 and miR-181b bindings with Ago1 protein complex.

$Gr1^+CD11b^+$ cells were isolated from the bone marrow of late septic mice. **(A–B)** HuR and Ago1 proteins bind miR-21 and miR-181b. Cell lysates were immunoprecipitated using A/G-agarose beads coated with antibody against HuR, Ago1 or IgG isotype control antibody. RNA was extracted from the immunoprecipitates (IP) using miRNeasy kit, and levels of miR-21 and miR-181b were determined by RT-qPCR using miScript SYBR Green PCR kit assay primers specific to miR-21 and miR-181b. Values were normalized to U6 RNA. **(C)** Ago1 is not involved in HuR binding to miR-21 and miR-181b. The $Gr1^+CD11b^+$ cells were transfected with Ago1-specific or control siRNAs and cultured for 36 hr. Cell lysates were immunoprecipitated with HuR antibody, and levels of miR-21 and miR-181b were determined as in *A*. **(D)** HuR promotes Ago1 binding of miR-21 and miR-181b. The $Gr1^+CD11b^+$ cells were transfected with HuR-specific or control siRNAs and cultured for 36 hr. Cell lysates were immunoprecipitated with Ago1-specific or IgG control antibody.

Levels of miR-21 and miR-181b in the immunoprecipitated protein complexes were determined by RT-qPCR as in *A*. Data in *A*, *B*, *C* and *D* are means ± SD of three experiments (n = 5–7 mice per group) and presented relative to the IgG IP sample (set at 1-fold). IP, immunoprecipitation. **(E)** HuR does not *affect* total cellular miR-21 and miR-181b levels. The $Gr1^{+}CD11b^{+}$ cells were transfected with HuR-specific or control siRNAs and cultured for 36 hr. Total RNA was isolated RNeasy kit, and levels of miR-21 and miR-181b were determined by RT-qPCR as in *A*. Data are means ± SD of two experiments (n = 5 mice per group) and are presented relative to control siRNA (1-fold). **(F)** HuR forms a protein complex with Ago1. $Gr1^{+}CD11b^{+}$ cell lysates were immunoprecipitated with HuR or IgG control antibody and immunoblotted with HuR or Ago1 antobody. The results are representative of two experiments.

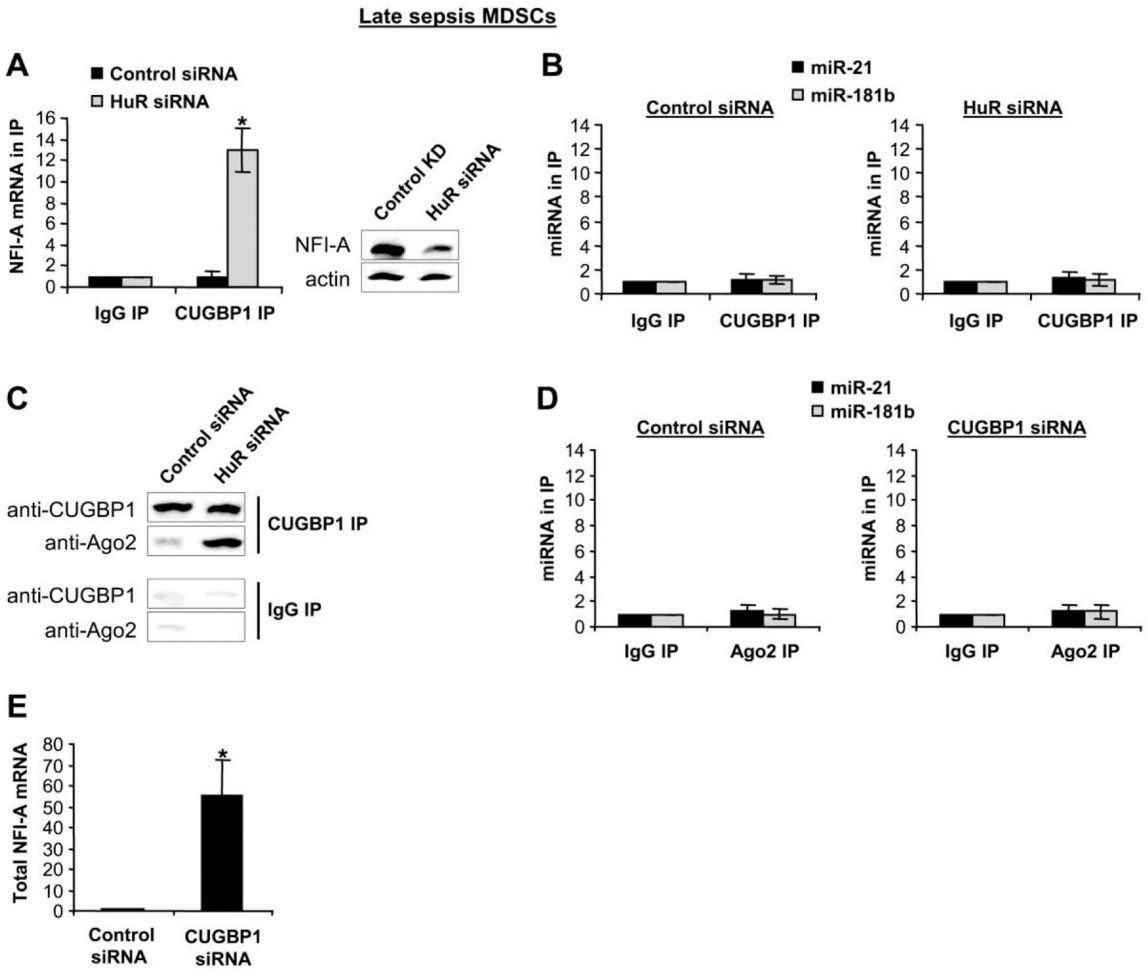

Figure 5: CUGBP1 protein binding to NFI-A mRNA in the absence of HuR.

$Gr1^+CD11b^+$ cells were isolated from the bone marrow of late septic mice. **(A)** CUGBP1 binds NFI-A mRNA after HuR knockdown. The cells were transfected with HuR-specific or control siRNAs and cultured for 36 hr. Cell lysates were immunoprecipitated with antibody against CUGBP1 or IgG control. RNA was extracted from the immunoprecipitates (IP) using TRIzol reagent and levels of NFI-A mRNA in the IP were measured by RT-qPCR using primers that amplify the 3ÙTR sequence. Values were normalized to GAPDH mRNA. NFI-A protein levels in whole cell lysate were determined by western blot using anti-NFI antibody. **(B)** CUGBP1 does not bind to miR-21 and miR-181b. RNA was extracted from CUGBP1 immunoprecipitates using miRNeasy kit, and levels of miR-21 and miR-181b were measured by RT-qPCR using miScript assay primers. Values were normalized to U6 RNA. **(C)** CUGBP1 forms a protein complex with Ago2 in the absence of HuR. The $Gr1^+CD11b^+$ cells were transfected with HuR siRNAs as in *A*. Cell lysates were immunoprecipitated with CUGBP1 or IgG control antibody and immunoblotted with CUGBP1 or Ago2 antibody. The results are representative of three experiments. **(D)** MiR-21 and miR-181b do not bind Ago2. The $Gr1^+CD11b^+$ cells were transfected with CUGBP1-specific, or control siRNAs and cultured for 36 hr. Cell lysates were immunoprecipitated with Ago2 or IgG control antibody. Levels of miR-21 and miR-181b in the IP was

determined as in *B*. (**E**) Knockdown of CUGBP1 increases NFI-A mRNA stability in the absence of miR-21 and miR-181b. The $Gr1^+CD11b^+$ cells were simultaneously transfected with miR-21 and miR-181b inhibitors as well as CUGBP1-specific or control siRNAs, and cultured for 36 hr. Total RNA was isolated, and levels of cellular NFI-A mRNA were measured by RT-qPCR using primers that amplify the 3ÙTR sequence and normalized to GAPDH mRNA. Data are means ± SD of 6 mice per group and are presented relative to control siRNA (1-fold). Data in *A*, *B* and *D* are means ± SD of three independent experiments (n = 6–7 mice per group) and are presented relative to the IgG IP sample (1-fold). $*p < 0.05$ vs. control siRNA. IP, immunoprecipitation.

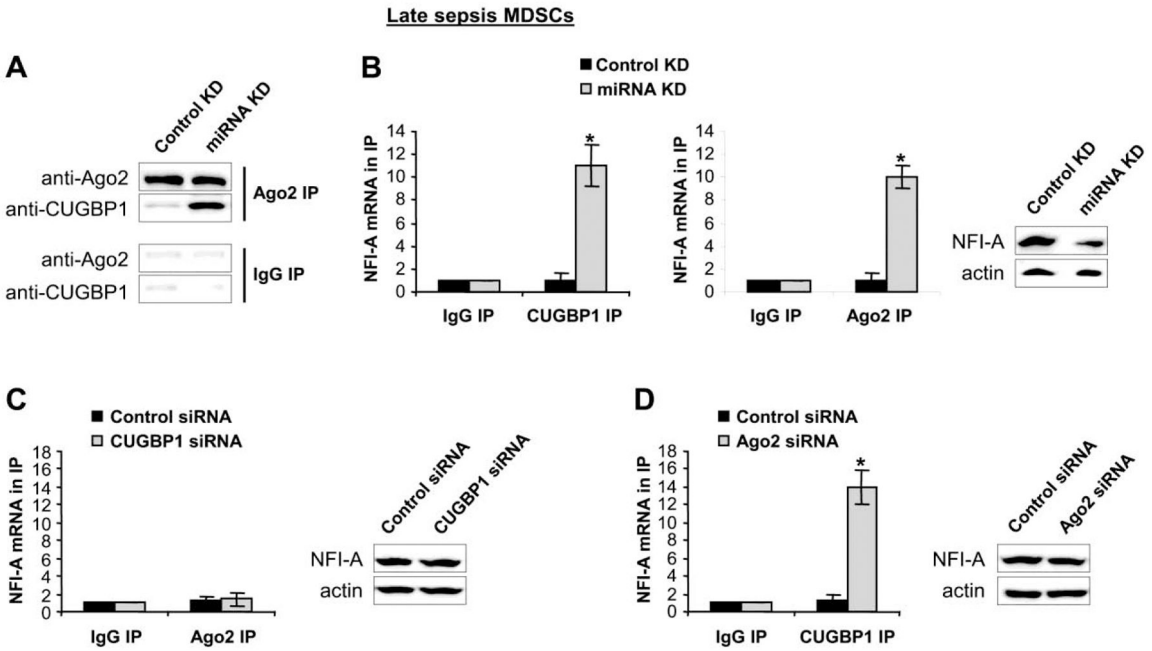

Figure 6: CUGBP1 interactions with and recruitment of Ago2 to NFI-A mRNA.

$Gr1^+CD11b^+$ cells were isolated from the bone marrow of late septic mice, transfected with miR-21 and miR-181b inhibitors or negative control inhibitors, and cultured for 36 hr. (**A**) CUGBP1 associates with Ago2 in the absence of the miRNAs. Cell lysates were prepared and immunoprecipitated with CUGBP1 or IgG control antibody, and immunoblotted with CUGBP1 or Ago2 antibody. The results are representative of two experiments. (**B**) To assess CUGBP1 or Ago2 binding to NFI-A mRNA, the cell lysates were immunoprecipitated with CUGBP1, Ago2 or IgG isotype control antibody. RNA was extracted from the immunoprecipitates (IP) using TRIzol reagent, and levels of NFI-A mRNA were measured by RT-qPCR using primers that amplify the 3ÙTR sequence. Values were normalized to GAPDH mRNA. Data are means ± SD of three experiments (n = 4–7 mice per group). *$p <$ 0.05 vs. control KD. **(C-D)** CUGBP1 recruits Ago2 to NFI-A 3'UTR. The $Gr1^+CD11b^+$ cells were simultaneously transfected with miR-21 and miR-181b inhibitors as well as CUGBP1-, Ago2-specific or control siRNAs, and cultured for 36 hr. Cell lysates were immunoprecipitated, and levels of NFI-A mRNA in the IPs were measured as in *B*. Data are means ± SD of three independent experiments (n = 6–8 mice per group) and are presented relative to the IgG IP sample (1-fold). *$p < 0.05$ vs. control siRNA. Right panels in *B*, *C* and *D* show NFI-A protein levels in whole cell lysates as determined by western blot using anti-NFI antibody. The results are representative of three experiments. IP, immunoprecipitation. KD, knockdown.

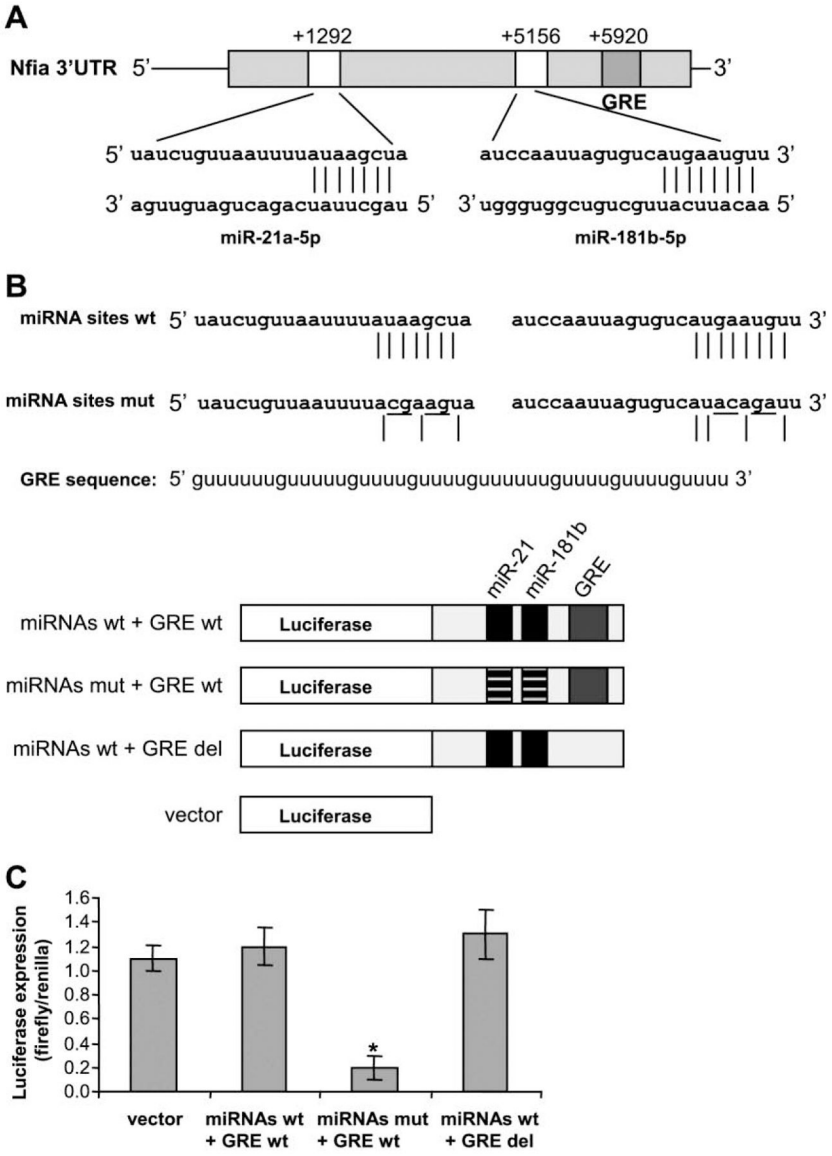

Figure 7: MiR-21 and miR-181b effect on reporter mRNA in sepsis Gr1$^+$CD11b$^+$ cells.

(**A**) A schematic representation of the NFI-A 3'UTR (7.641 kb), which spans the region from +1634 to +9274 of the mRNA sequence, with locations of miR-21 and miR-181b binding sites and GRE element. (**B**) Sequences of the miR-21 and miR-181b as well as the GRE are shown. Mutations introduced in the miRNA binding sites are underlined. A 4.906 kb fragment (from +1168 to +6074) of NFI-A 3'UTR containing the miRNA binding sites and the GRE element was cloned in the pEZX-MT06 dual firefly and *Renilla* reporter vector downstream of firefly luciferase. Diagrams of the luciferase constructs with the miRNAs and GRE locations are shown. GRE, GU-rich element; wt, wild-type; mut, mutant; del, deleted. (**C**) Gr1$^+$CD11b$^+$ cells were isolated from the bone marrow of late septic mice. The cells were transfected with indicated luciferase constructs. After 36 hr, cells were harvested for the measurement of firefly and *Renilla* luciferase activities. A luciferase vector without the NFI-A 3'UTR insertion served as a positive control. Firefly luciferase values were

normalized to *Renilla* luciferase activity and are presented as a firefly/*Renilla* ratio. Data are expressed as means ± SD of three experiments (n = 4–6 mice per group). *$p < 0.05$. Wt, wild-type; mut, mutant.